THE STRUCTURAL DESIGN OF TALL AND SPECIAL BUILDINGS
Struct. Design Tall Spec. Build. (2008)
Published online in Wiley Interscience (www.interscience.wiley.com). **DOI**: 10.1002/tal.468

NONLINEAR SEISMIC RESPONSE OF MILAD TOWER USING FINITE ELEMENT MODEL

MAHMOOD YAHYAI*, BAHRAM REZAYIBANA AND AMIR SAEDI DARYAN
Department of Civil Engineering, K. N. Toosi University of Technology, Tehran, Iran

SUMMARY

Milad Tower is a 436-m-tall telecommunications tower ranked as the fourth tallest structure of its kind in the world. The study of its seismic behaviour is of great importance as it is located in a highly seismic-prone region. Because of the existence of the world's largest revolving restaurant in the head structure, and also because of the highly sensitive communication devices such as TV and telecommunications antennas installed on the tower, nonlinear deformation under future earthquakes should be studied. In this paper, a detailed finite element model is developed and nonlinear dynamic analysis was carried out under the design earthquakes. The foundation, concrete shaft, head structure and 120-m antenna structure were modelled. Three components of the earthquakes are considered, and the selected earthquakes were normalized based on three design levels: design basis level, maximum design level and maximum credible level. The results of the analysis showed that all parts of the tower behave in the plastic zone except the elements of the head structure. It is also observed that in some cases, the earthquakes with lower peak accelerations and higher energy contents may have more severe effect on the tower than that with higher peak accelerations. Copyright © 2008 John Wiley & Sons, Ltd.

1. INTRODUCTION

The study of the seismic behaviour of a telecommunications tower needs an accurate finite element modelling. Two methods are usually used to study the response of tall towers. In the first method, called stick model, the behaviour of the tower is assumed as a cantilever beam with variable sections. The structure is divided into a number of parts at different levels, and the geometrical and material properties are defined for each part. As many structural details are simplified and neglected in this method, only the overall behaviour of the structure can be obtained. The foundation is not considered and the head structure is simulated by concentrated masses in this method.

In the second method, finite element models are developed using suitable software. Since the number of degrees of freedom is high, the analysis is time-consuming, and enormous calculations should be carried out when the nonlinear properties of materials are considered.

Many researches have been carried out to study the seismic behaviour of tall buildings. Riva *et al*. (1998) used the finite element model in the nonlinear dynamic analysis of Asinelli Tower in Bologna. They used a simple finite element model to study the behaviour of the tower under dynamic loadings. Halabian *et al*. (2002) used a simplified pseudo-dynamic analysis procedure for the soil–structure analysis of free-standing towers with multiple nonlinearities in the cross-sections due to earthquakes. They studied the effects of the foundation flexibility, cracking and yielding in the concrete members

*Correspondence to: Mahmood Yahyai, K. N. Toosi University of Technology, PO Box 15875-4416, Tehran, Iran. E-mail: yahyai@kntu.ac.ir

on the dynamic response of the structure. They concluded that when the ductile behaviour of the tower is considered in the design, the lateral response of the structure is more sensitive to the cracking and yielding in the reinforced concrete members than to the foundation flexibility. Horr *et al*. (2002) analysed Tehran Telecommunication Tower by using fractional modulus. They used advanced complex damped spectral element method with more accurate and mathematically complicated shape functions in their research. They concluded that this method can accurately predict the frequency-dependent dynamic characteristics of the reinforced concrete tower. Khaloo *et al*. (2001) studied the linear and nonlinear responses of Milad Tower using three different finite element models. Cracking and crushing of the reinforced concrete material and large deformation effects were considered in their study. They concluded that there is a good agreement between the results of the stick models and the solid concrete models. In this paper, the finite element program ABAQUS is used to conduct the dynamic analysis of Milad Tower. A detailed three-dimensional (3-D) finite element model of the tower is developed, and three components of six selected earthquakes are simultaneously applied to the model. This kind of finite element modelling is carried out for the first time for the structure of Milad Tower.

2. STRUCTURE OF MILAD TOWER

Milad Tower consists of five main parts: foundation, transition structure, concrete shaft, head structure and the antenna mast.

2.1 Foundation

The foundation of the tower consists of two parts: the circular mat foundation and the transition structure. The diameter of the mat foundation is 66 m, and the thickness is varied between 3 and 4·5 m. The transition structure is a truncated pyramid placed on a mat foundation and continued until the height level of 0·0 m. The diameter of the transition structure is 28 m. This structure consists of a central core, inclined walls and triangular-shaped walls. To control the stresses under the foundation, as well as the punching shear, a post-tensioning system is used around the foundation to provide compression in the foundation as well as in the concrete confinement. The different parts of the foundation are shown in Figure 1.

2.2 Concrete shaft

The concrete shaft is the main load-carrying structure of the tower that transfers all of the lateral and gravitational loads to the foundation. This structure begins from the height level of 0·0 m to the height level of 315 m. This part consists of four tapered walls with trapezoidal and two interconnected octagons that are connected by several walls. The sections of the four tapered walls with trapezoidal are variable in the height of the structure and are decreased along the height of the tower. At the height level of 0·0 m, the diameter of the main body is 28 m, which is decreased to 18·2 m at the height level of 233 m. To increase the bending capacity of the tower at the height levels over 240 m, and also to decrease the mast displacement, the exterior and the interior octagons are post-tensioned at the height levels of 230–302·4 m and 290–315 m, respectively. The cross-section of the concrete shaft at different height levels are shown in Figure 2.

2.3 Head structure

The head structure begins at the height level of 247·5 m and is continued until the height level of 315 m. It is placed around the concrete shaft and forms a 12-storey structure. A space basket is placed

DOI: 10.1002/tal

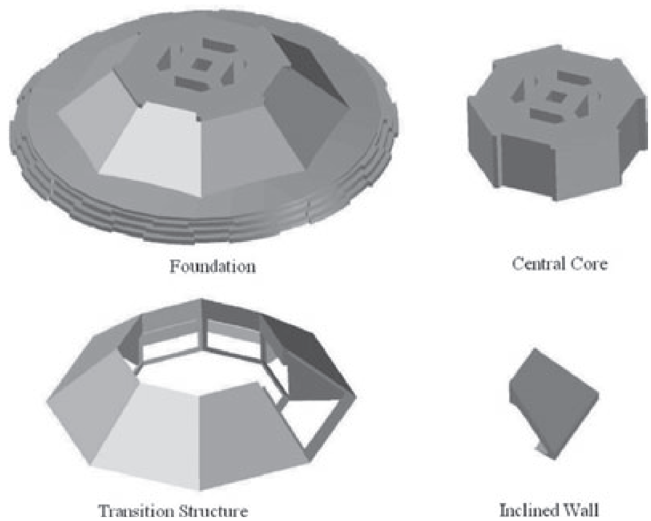

Figure 1. Foundation of Milad Tower

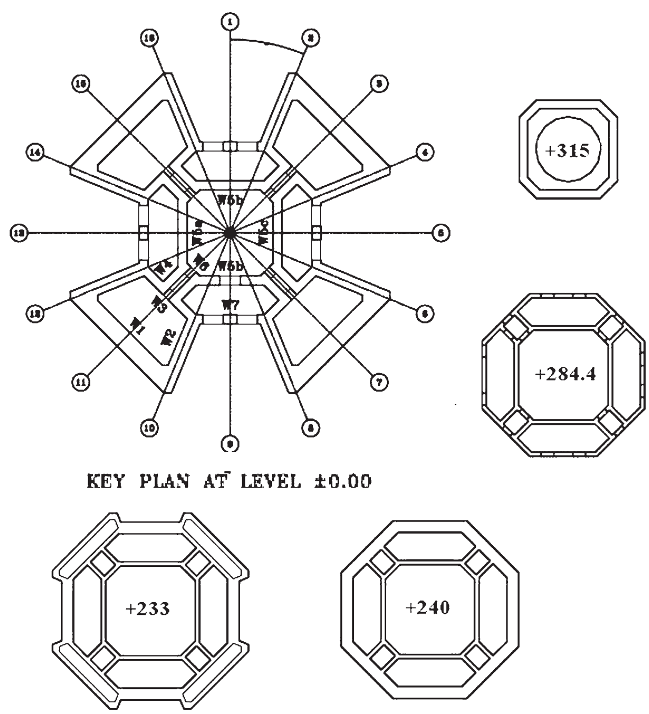

Figure 2. The cross-section of the concrete shaft at different elevations

DOI: 10.1002/tal

around the head structure at the height levels of 254·4–280·8 m. A sky dome is also placed at the height range of 302·4–313·25 m. The main parts of the head structure are radial and peripheral beams, columns, basket, and concrete shaft.

The radial beams are placed between the columns or between the columns and the concrete shaft and transfer the load of joists to the columns or the concrete shaft. The peripheral beams are placed on the perimeter of the structure and transfer the loads to the columns.

The columns transfer the loads to the columns or the basket and are finally transmitted to the concrete shaft. The columns of the head structure are classified into four groups:

(1) Base column: This column transfers the main part of the head structure loads (except the small portion of load that is directly transferred to the main body) to the concrete shaft.
(2) C1 column: This column begins from the height level of 254·4 m and is continued to the height level of 302·4 m. The radius of the placement of this column is 12·4 m, and the column is connected to the base column at the height level of 254·4 m.
(3) C2 column: This column begins from the height level of 261·6 m with a radius of 12·4 m and reaches the height level of 271·2 m with a radius of 17 m, and then continues to the height level of 297·6 m with a constant radius. This column is connected to the C1 column at the height level of 261·6 m to transfer its load.
(4) C3 column: This column begins from the height level of 274·5 m and ends at the height level of 288 m. The placement radius of this column is 24·96 m.

The basket is placed around the head structure from the height level of 254·4 m to the height level of 280·8 m. The basket is attached to the structural elements of the head structure at all elevations except at the height level of 266·5 m.

The concrete cone is constructed from the height level of 247·5 m to the height level of 254·4 m. This structure participates in load transferring due to its significant thickness and continuity. The inclined base columns of the head structure have significant axial forces. The horizontal component of these axial forces creates high tensile forces in the radial beams and the concrete slab at the height level of 254·4 m. These tensile forces are significant, and to overcome these forces, a post-tensioned peripheral beam is designed at this level. The head structure is shown in Figure 3.

2.4 Antenna mast

One of the main parts of a telecommunications tower is the antenna mast. The antenna is installed from the height level of 308 m to the height level of 436 m. It is composed of four parts.

(1) The first part is installed from the height level of 308 m to the height level of 382 m. The diameter of this part is 6 m at the height range of 308–315 m and is decreased to 3·5 m at the highest part.
(2) The second part is installed from the height level of 382 m to the height level of 408 m. The section of this part is an irregular octagon, and the exterior diameter is 1·9 m.
(3) The third part is installed from the height level of 408 m to the height level of 420·8 m. The section of this part is also an irregular octagon, and the exterior diameter is 1·3 m.
(4) The fourth part is installed from the height level of 420·8 m to the height level of 436 m. The section of this part is a square, and the exterior diameter is 0·6 m.

3. FINITE ELEMENT MODEL

Eight-node solid elements are used to model the circular foundation and the central part of the transition structure. Triangular shell elements and four-node shell elements are used for modelling the

DOI: 10.1002/tal

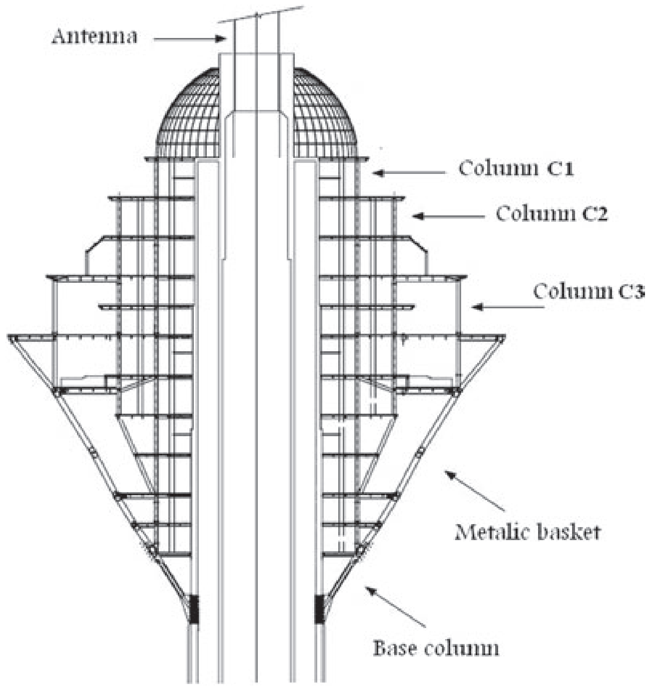

Figure 3. The head structure of Milad Tower

triangular and inclined walls, respectively. Three-dimensional truss elements are used for modelling the post-tension tendons that are embedded in the exterior ring of the circular foundation. Reinforcements are accurately placed in the finite element model according to the structural drawings.

Four-node shell elements are used from the height level of 0.0 m to the height level of 307 m, where the section of the shaft is changed to accommodate the antenna mast. Eight-node solid elements are used above the height level of 307 m for modelling the concrete shaft. The concrete shaft is modelled accurately with every structural part.

All members of the head structure are modelled using a 3-D Bernoulli–Euler beam, in which the shear deformation is ignored. To consider the floor rigidity, all of the nodes are tied together in every storey to have equal movements (equal transition in the X and Y directions and equal rotation about the Z-axis.

Four-node shell elements are used for modelling the antenna mast, and the stiffeners are modelled by 3-D Bernoulli–Euler beam elements. This part is also modelled completely. The finite element of the tower is shown in Figure 4. It should be mentioned that the finite element model consists of 13 284 elements and 17 920 nodes.

4. MATERIAL MODELLING

The materials used in the structure are mainly steel and concrete, and convenient models are used to define the behaviour using the ABAQUS software (ABAQUS, 2006).

DOI: 10.1002/tal

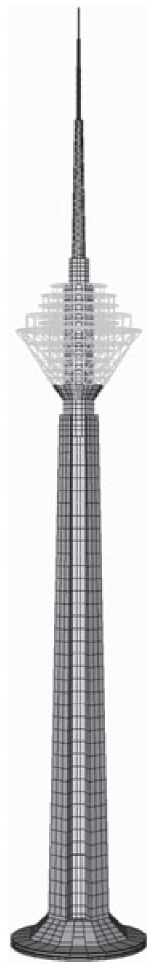

Figure 4. Finite element of Milad Tower

4.1 Steel

The isotropic trilinear steel model is used for high-strength steel, and the isotropic bilinear steel model is used for tendons and high-strength bars that do not have a plastic plateau (Table 1).

4.2 Concrete

The 28-day compressive strength of the concrete used in the foundation and the concrete shaft is reported as 35 MPa. The damaged plasticity model is used to simulate the behaviour of concrete in the tower (Table 2).

5. SEISMIC LOADING

Selected earthquake accelerograms are scaled for the required design levels to conduct a time history analysis. The accelerograms should be scaled in such a way that the obtained spectrum is similar to

DOI: 10.1002/tal

Table 1. Mechanical properties of the steels

Steel grade	Yield stress (MPa)	Ultimate stress (MPa)	Ultimate strain	Module of elasticity (10^5 MPa)
A-III bar	400	600	0·14	2·1
Special bar	500	650	0·1	2·1
A416-grade 270 tendon	1600	1860	0·04	1·96
Steel plate ST37	240	370	0·28	2·1
Steel plate ST52	350	520	0·22	2·1
Steel plate 480AT	500	690	0·14	2·1

Table 2. Properties of the concrete

Poison coefficient	Compressive yield stress (MPa)	Compressive ultimate stress (MPa)	Tensile strength (MPa)	Module of elasticity (MPa)
0·167	24·02	32·36	1·78	26 480

Table 3. The selected earthquake accelerograms for the different design levels

Design level	Earthquake accelerogram	Station	Horizontal PGA (g)	Horizontal PGA (g)	Vertical PGA (g)
DBL	Ghaen, Iran, 27 September 1979	Ghaen	0·30	0·29	0·23
DBL	Parkfield, CA, 27 June 1966	Cholame Shandon 5	0·31	0·29	0·19
MDL	Irpinia, Italy, 23 November 1980	Brienza	0·47	0·44	0·33
MDL	Smart Array event, 30 July 1986	C—∞	0·51	0·49	0·36
MCL	Kern County, 21 July 1952	Taft	0·63	0·58	0·43
MCL	Manjil, Iran, 20 June 1990	Ab-bar	0·56	0·55	0·49

the one assumed for that specific design level. In the seismic hazard analysis of Milad Tower, selecting and scaling of the earthquake accelerograms are made considering the peak ground acceleration (PGA), frequency content, enduring time and geotechnical properties. For each design level, the Fourier spectrum of the original accelerogram is first calculated, and then the scaling is conducted considering the ratio of the required response spectrum to the original accelerogram response spectrum. This operation is carried out in such a way that the final response spectrum obtained agrees well with the required response spectrum. Scaling operations are done considering 5% for damping. For each design level, two earthquake accelerograms having two horizontal and one vertical components are selected. These accelerograms are tabulated in Table 3.

The peak accelerations mentioned in Table 3 are related to the normalized accelerograms.

6. MODAL ANALYSIS

To calculate the Rayleigh damping coefficients for the dynamic analysis, it was necessary to conduct a modal analysis. The results of the modal analysis are shown in Table 4. Since the structure has approximately symmetric modes, the vibrating mass of a real mode is divided into two symmetric modes in the X and Y directions and only half of the corresponding vibrating mass oscillates in each mode. Hence, the vibrating mass of two symmetric modes is related to one vibration mode.

The eigenvalues are obtained by calculating the average value of the two symmetric modes, and the effective mass is calculated as the summation of those vibrating mass. It can be seen from Table 4 that more than 90% of the mass vibrates in the first 10 vibration modes, which confirms the correct

DOI: 10.1002/tal

Table 4. Modal analysis of Milad Tower

Mode number	Eigenvalue	Period (s)	Effective mass (10^3 kg)	Rotation frequency (cycles/s)	Angular frequency (rad/s)
1	0·7346	7·330	100 086	0·13641	0·85710
2	8·3654	2·172	2270	0·46032	2·85810
3	19·3358	1·429	39 970	0·6999	4·3976
4	52·9114	0·846	1587	1·1577	7·2742
5	105·9150	0·611	18 538	1·6379	10·2915
6	229·3000	0·416	905	2·4050	15·1410
7	323·0900	0·350	11 180	2·8610	17·9750
8	468·5200	0·290	1919	3·4449	21·6450
9	753·2850	0·229	965	4·3681	27·4460
10	779·6150	0·225	3486	4·4440	27·9210

selection of the vibration modes. The first, third, fifth and seventh modes are the main vibration modes of the tower that have the most effect on the behaviour of the structure. It can be seen from Table 4 that 50·71% of the tower mass vibrates in the first vibration mode, but the upper modes also have significant importance. The two first modes are used for calculating the Rayleigh damping coefficients (Chopra AK, 1991). The Rayleigh coefficients are calculated by Equation (1).

$$\begin{Bmatrix} \xi_1 \\ \xi_2 \end{Bmatrix} = \frac{1}{2}\begin{bmatrix} \dfrac{1}{\omega_1} & \omega_1 \\ \dfrac{1}{\omega_2} & \omega_2 \end{bmatrix} \tag{1}$$

Considering a damping of 5% for the first two major modes and the frequencies of the first two modes, $\omega_1 = 0{\cdot}8571$ and $\omega_2 = 4{\cdot}398$, the Rayleigh damping coefficients were calculated as $\alpha = 0{\cdot}071$ and $\beta =$ 0·071 for the first two major modes, respectively. The shapes of the first two modes are shown in Figure 5.

7. TIME HISTORY ANALYSIS

The selected earthquakes are applied to the tower. Since the overall structural, material and loading details are precisely considered in the finite element model, all of the three components of earthquakes are applied to the structure simultaneously. The nonlinear seismic analyses for the 3-D model are performed, and the results are compared for the three FE models (Rezaeibana, 2008).

7.1 Base shear and overturning moment

The maximum shears and moments at the height levels of 0·0 m and −14·00 m are presented in Table 5. The following results can be concluded from Table 5.

Both selected earthquakes have approximately equal values for shear and moment in the design basis level (DBL) since they create a similar force on the tower. Consequently, an average value of shear and moment can be used for design purposes.

In the maximum design level (MDL), the moments in the *Y* direction are significantly different for the Smart Array earthquake. There is also a significant difference between the moment in the *X* and *Y* directions. The main cause of these differences may be the nature of the record in the *X* direction. The earthquake record has subsequent acceleration peaks that are suddenly applied to the structure,

DOI: 10.1002/tal

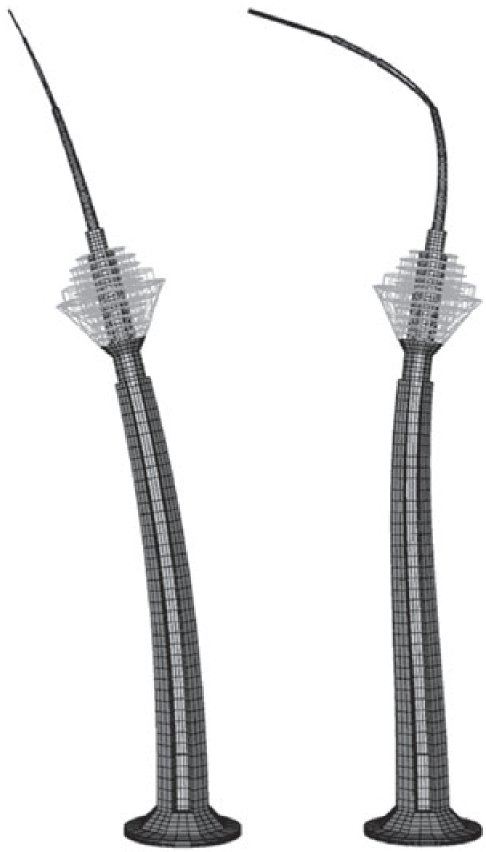

Figure 5. Modal analysis of Milad Tower

Table 5. Shear force and bending moment values at −14- and 0.0-m levels

MCL		MDL		DBL		
Manjil	Kern County	Irpinia	Smart	Parkfield	Ghaen	Design level
6·21	7·52	5·49	5·50	3·27	3·10	Base shear X (10^8 N)
6·72	7·66	5·54	6·03	3·18	3·23	Base shear Y (10^8 N)
13·42	12·12	8·66	8·92	8·12	8·33	Base moment X (10^9 N·m)
14·4	9·59	8·74	10·22	7·95	8·28	Base moment Y (10^9 N·m)
1·57	1·85	1·31	1·81	1·05	1·15	Shear at 0·0-m level X (10^8 N)
1·76	1·79	1·48	1·89	0·92	0·92	Shear at 0·0-m level Y (10^8 N)
11·09	10·27	7·58	7·77	8·06	7·15	Moment at 0·0-m level X (10^9 N·m)
11·52	9·00	7·27	9·76	6·98	7·82	Moment at 0·0-m level Y (10^9 N·m)

DOI: 10.1002/tal

and it seems that these sudden impacts increase the response of the structure in one direction (Figure 6). Base moment in the *Y* direction is shown in Figure 7.

In the maximum credible level (MCL), there are significant differences between the responses of the structure to the earthquake records. Manjil earthquake is a near-field earthquake and several acceleration pulses exist in all of the three components of the earthquake, which cause a large amount of energy to the structure.

The ratios of the base shear and moment to the shear and moment at the height level of 0·0 m are listed in Table 6. It can be seen that the base shear is significantly greater than the shear at the height level of 0·0 m. It can be concluded that a great amount of shear is applied to the foundation. This shows that to obtain accurate results, the effect of the foundation on the seismic behaviour of structure should be considered.

7.2 *Overall deformation of the tower*

Deformations of the tower in different design levels were studied. Since the stiffness of the mast is much less than the stiffness of the concrete shaft, the largest displacement occurred in the mast. The

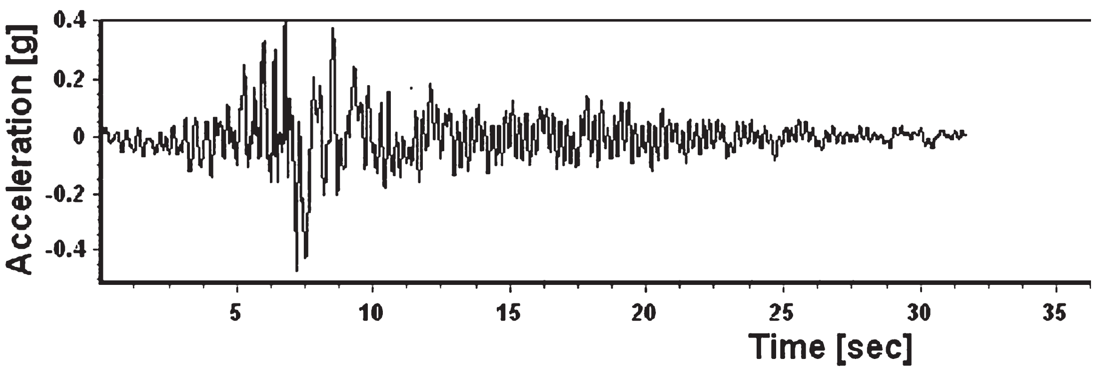

Figure 6. X-component of Smart Array accelerogram

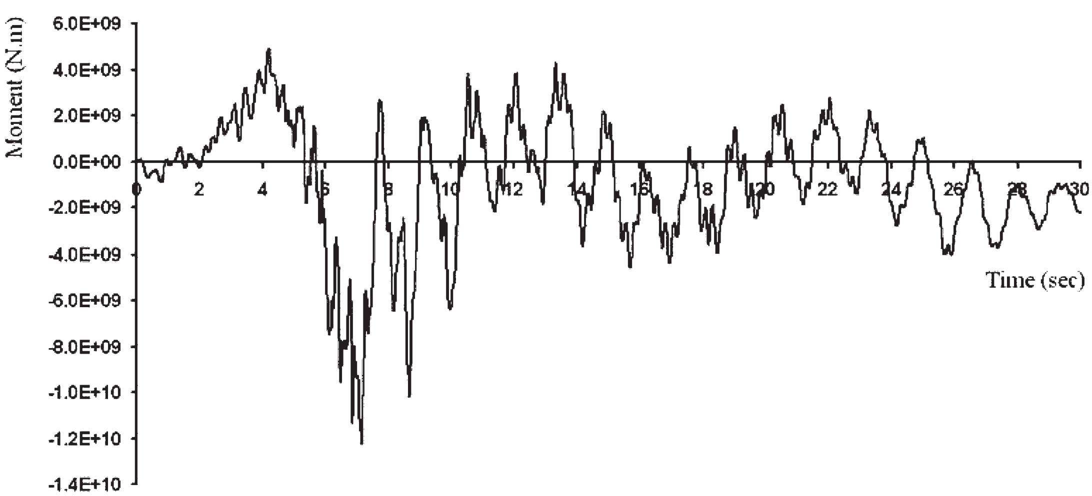

Figure 7. Base moment–time history in the *Y* direction due to the Smart Array earthquake

DOI: 10.1002/tal

Table 6. Average values of shear and moment

MCL	MDL	DBL	Design level
70 000	58 000	32 000	Base shear (ton)
17 500	16 000	10 000	Shear at 0·0-m level
4·00	3·63	3·2	Base/0·0-m level shear ratio
1 240 000	920 000	820 000	Base moment (tonne.m)
1 050 000	810 000	750 000	0·0-m level moment (tonne metre)
1·18	1·01	1·09	Base/0·0-m level moment ratio

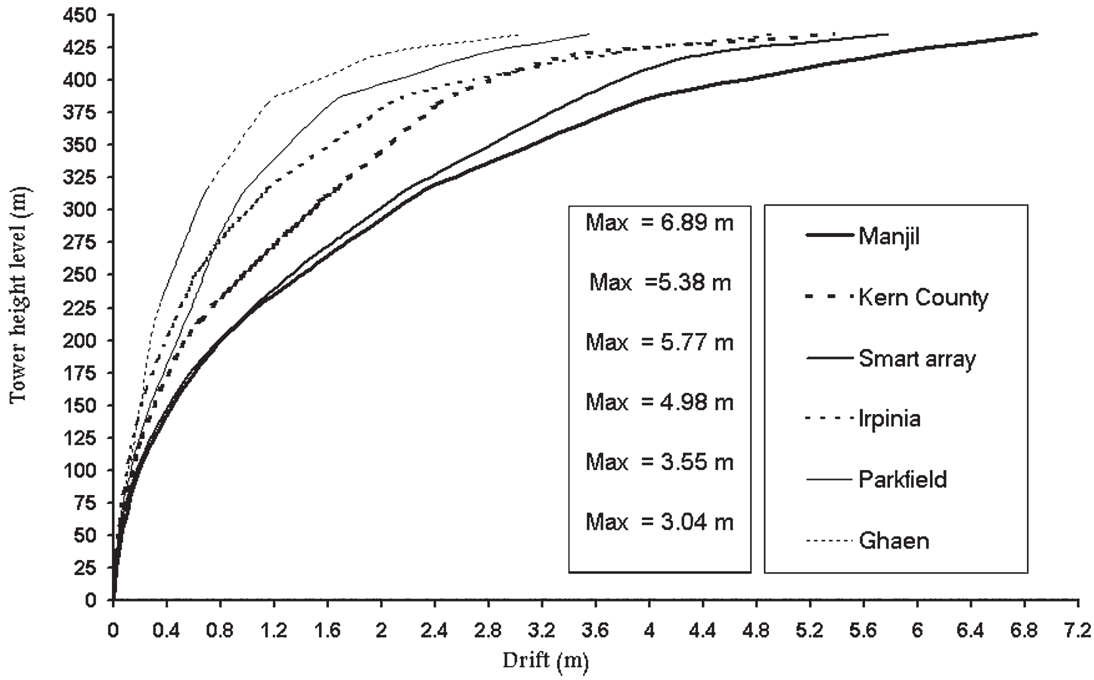

Figure 8. Tower displacement in the *X* direction

displacements of the tower at different levels are studied and are shown in Figures 8 and 9, respectively. The tower deforms like a cantilever beam and the displacement increases at higher height levels. Below the height level of 100 m, all the displacements are linear; but at upper levels, due to the plastic deformation and the variation of the cross-section of the tower, the deformations are nonlinear. The displacement is significant above the elevation of 315 m.

The maximum displacement of the tower at the height levels of 315 and 435 m for the different design levels are shown in Table 7.

As it can be seen from Figure 8, the displacement of the tower in the *X* direction due to the Smart Array earthquake is more than the displacement of Iripinia caused by the same design level MDL, and is even more than the displacement of Kern County caused by the higher design level MCL. When several acceleration peaks are suddenly imposed to the structure, a great amount of energy is applied and the structure could not damp this amount of energy in a short period of time, and consequently, the response of the structure increases.

DOI: 10.1002/tal

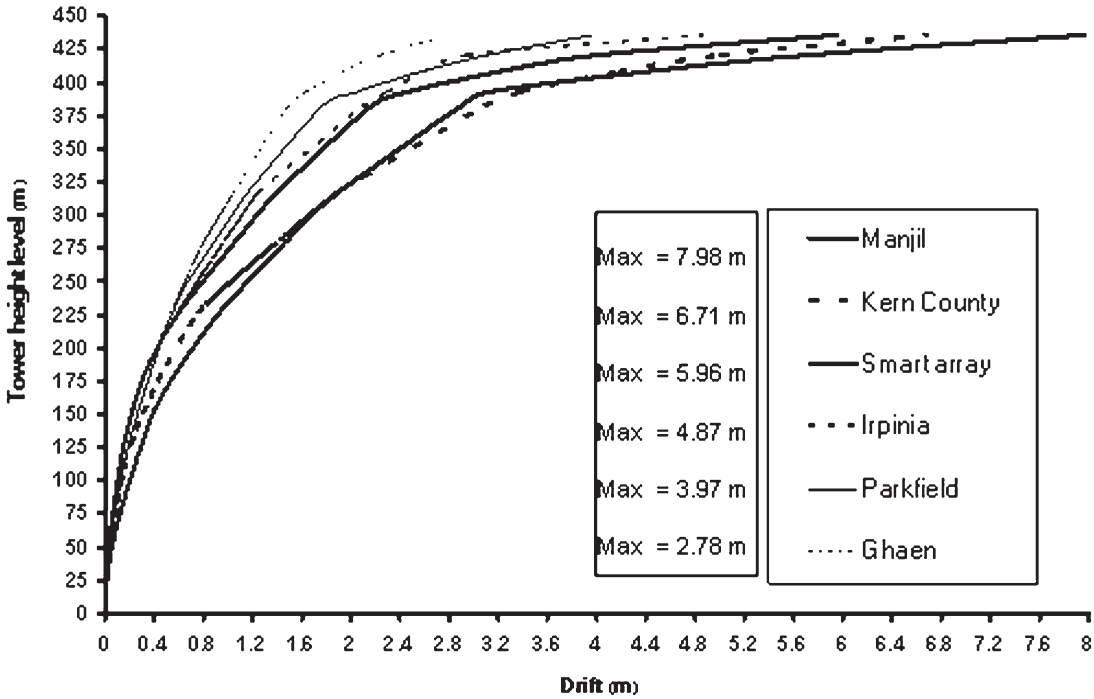

Figure 9. Tower displacement in the *Y* direction

Table 7. Displacement of Milad Tower at different design levels and height levels

Height level (m)	DBL (m)	MDL (m)	MCL (m)
315	0·96	1·48	1·92
436	3·34	5·40	6·75

As it can be seen from Figure 10, a great amount of energy is applied to the structure in the Smart Array earthquake in 5 s (66% of total earthquake energy), whereas 26% of total energy is applied to the tower in the Kern County earthquake. The Arias Intensity used for comparing the two earthquake energies is as follows:

$$I_a = \frac{\pi}{2g}\int_0^{\infty}[a(t)]^2 dt \qquad (2)$$

7.3 *Forces in the head structure*

The head structure and the concrete shaft vibrate together in that significant forces appear due to the horizontal component of the earthquakes. Considerable forces occur in the head structure due to the vertical component of the earthquakes.

The maximum stresses in the structural members of the head structure are listed in Table 8. Percentages of stress in the members due to the vertical component of the earthquakes are presented in Table 9. It can be seen that stresses in the members are less than the allowable stress. Although the stresses

DOI: 10.1002/tal

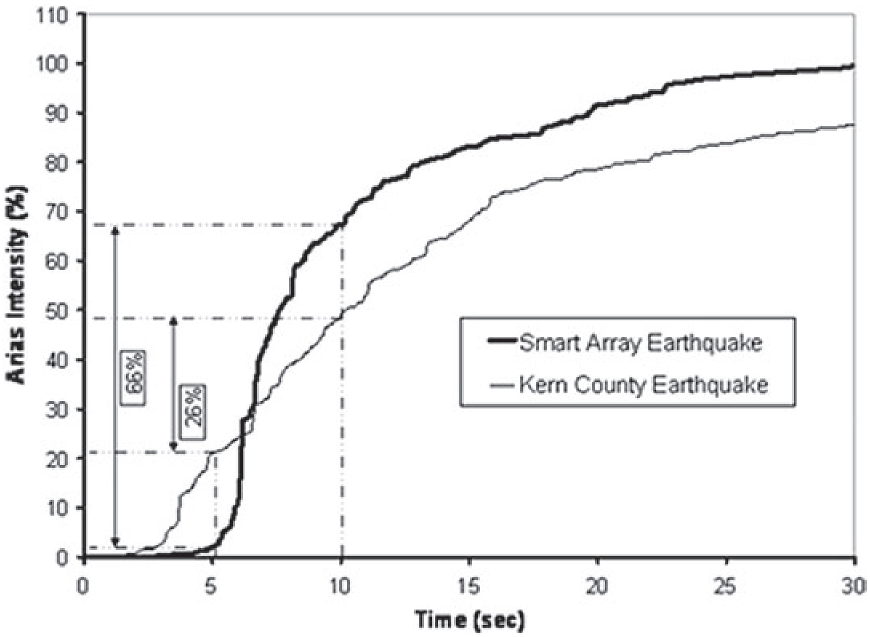

Figure 10. Percentages of the Arias Intensity of the Kern County and Smart Array earthquakes

Table 8. Maximum stress in the head structure members (MPa)

Manjil	Kern County	Smart Array	Iripinia	Parkfield	Ghaen	Member
86	84	85	93	74	72	Base column
206	206	206	204	160	164	C1 column
298	257	267	302	240	276	Radial beam
168	154	156	154	122	120	Basket members

Table 9. Additional stress percentage in the head structure members

Manjil	Kern County	Smart Array	Iripinia	Parkfield	Ghaen	Member
80	80	80	80	40	40	Base column
80	80	80	80	40	40	C1 column
84	58	65	86	50	66	Radial beam
120	95	98	97	56	55	Basket members

due to the vertical component of the earthquakes can be twice that of the horizontal component, all structural members remain in the elastic zone under the design earthquakes.

8. CONCLUSIONS

Although the interpretation of a nonlinear time history analysis for a huge structure such as Milad Tower is difficult, the general behaviour of the structure during future earthquakes can be predicted. The following brief results can be concluded.

DOI: 10.1002/tal

The ratio of the base shear to the shear force at ground level (0·0 m) for the tower was obtained approximately between 3 and 4 m, which indicate that high shear forces are developed in the foundation under earthquakes. This shows that the foundation should be modelled and that the cantilever beam model is an extreme assumption that could not lead to reliable results for such towers. Lateral displacement of the tower is linear up to the elevation height of 100 m; above that, the displacement is nonlinear. All of the members of the head structure remained in the elastic zone during the applied earthquake forces. Considering this fact, and to reduce the calculation time, the head structure can be modelled as lumped masses at the floor level.

ACKNOWLEDGEMENT

The structural and risk analysis reports provided by the Yadman Sazeh Co. to carry out this research is highly acknowledged.

REFERENCES

ABAQUS. 2006. *ABAQUS Theory Manual and Users' Manual, Version 6.6*. Hibbitt, Karlsson & Sorenson, Inc.

Chopra AK. 1991. *Dynamics of Structures: Theory and Applications to Earthquake Engineering* (2nd edn). Prentice-Hall: Englewood Cliffs, New Jersey.

Halabian AM, Naggar MH, Vickery BJ. 2002. Nonlinear seismic response of reinforced-concrete free-standing towers with application to TV towers on flexible foundations. *The Structural Design of Tall and Special Buildings* **11**: 51–72.

Horr AM, Safi M, Asadpour N. 2002. Seismic analysis of Tehran telecommunication tower using complex fractional modulus. *The Structural Design of Tall and Special Buildings* **11**: 353–374.

Khaloo AR, Asadpour N, Horr AM. 2001. Full dynamic analysis of Tehran telecommunication tower; linear and nonlinear responses. *The Structural Design of Tall and Special Buildings* **10**: 263–281.

Rezaeibana B. 2008. Nonlinear dynamic analysis of tall telecommunication towers. MS Thesis, K. N. Toosi University of Technology, Tehran, Iran.

Riva P, Perotti F, Guidoboni E, Boschi E. 1998. Seismic analysis of the Asinelli Tower and earthquakes in Bologna. *Solid Dynamics and Earthquake Engineering* **17**: 525–550.